Chemotactic Responses of *Escherichia coli* to Small Jumps of Photoreleased L-Aspartate

Ravi Jasuja,* Jinsoo Keyoung,* Gordon P. Reid,# David R. Trentham,# and Shahid Khan*
*Department of Physiology and Biophysics, Albert Einstein College of Medicine, Bronx, New York 10461 USA, and #National Institute for Medical Research, Mill Hill, London NW7 1AA, England

ABSTRACT Computer-assisted motion analysis coupled to flash photolysis of caged chemoeffectors provides a means for time-resolved analysis of bacterial chemotaxis. *Escherichia coli* taxis toward the amino acid attractant L-aspartate is mediated by the Tar receptor. The physiology of this response, as well as Tar structure and biochemistry, has been studied extensively. The β-2,6-dinitrobenzyl ester of L-aspartic acid and the 1-(2-nitrophenyl)ethyl ether of 8-hydroxypyrene-1,3,6-tris-sulfonic acid were synthesized. These compounds liberated L-aspartate and the fluorophore 8-hydroxypyrene 1,3,6-tris-sulfonic acid (pyranine) upon irradiation with near-UV light. Photorelease of the fluorophore was used to define the amplitude and temporal stability of the aspartate jumps employed in chemotaxis experiments. The dependence of chemotactic adaptation times on aspartate concentration, determined in mixing experiments, was best fit by two Tar aspartate-binding sites. Signal processing (excitation) times, amplitudes, and adaptive recovery of responses elicited by aspartate jumps producing less than 20% change in receptor occupancy were characterized in photorelease assays. Aspartate concentration jumps in the nanomolar range elicited measurable responses. The response threshold and sensitivity of swimming bacteria matched those of bacteria tethered to glass by a single flagellum. Stimuli of similar magnitude, delivered either by rapid mixing or photorelease, evoked responses of similar strength, as assessed by recovery time measurements. These times remained proportional to change in receptor occupancy close to threshold, irrespective of prior occupancy. Motor excitation responses decayed exponentially with time. Rates of excitation responses near threshold ranged from 2 to 7 s^{-1}. These values are consistent with control of excitation signaling by decay of phosphorylated pools of the response regulator protein, CheY. Excitation response rates increased slightly with stimulus size up to values limited by the instrumentation; the most rapid was measured to be 16 $\pm$ 3 (SE) s^{-1}. This increase may reflect simultaneous activation of CheY dephosphorylation, together with inhibition of its phosphorylation.

INTRODUCTION

Strong chemotactic responses are evoked by acidic amino acids in a wide variety of sensory systems ranging from bacteria to humans. Chemotaxis of the bacterium *Escherichia coli* toward amino acid chemoattractants provides a well-understood example of a single-cell sensory response (Berg, 1983; Blair, 1995; Stock and Surette, 1996; Appleby et al., 1996; Falke et al., 1997; Bray, 1998). The motility of these bacteria consists of an alternating pattern of swimming runs and tumbles. During runs, the six or so flagella per cell form a counterclockwise (CCW) rotating bundle that provides thrust. Reversal to clockwise (CW) rotation of an undetermined number of flagella breaks up the bundle, causing tumbling events that randomize cell orientation. Chemotactic migration is accomplished by increasing swimming runs up spatial, attractant gradients (Berg and Brown, 1972).

The smooth-swim response to L-aspartate is mediated by the Tar receptor, one of a family of transmembrane methyl-accepting chemotaxis proteins (MCPs) that mediate responses to diverse stimuli. Insights into Tar structure and its modulation by aspartate binding have been obtained by x-ray crystallography (Milburn et al., 1991), NMR (Danielson et al., 1994), and mutagenesis (Falke and Koshland, 1987; Cochran and Kim, 1996; Gardina and Manson, 1996). Motile responses to changes in extracellular aspartate concentration are effected by an intracellular signaling cascade composed of the chemotaxis proteins CheA, CheW, and CheY. Tar and other MCPs form complexes with the linker CheW and the histidine kinase CheA (Gegner et al., 1992). CheA, as part of such receptor complexes, phosphorylates CheY, forming CheY-P. CheY regulates motor rotation, binding to the motor when phosphorylated and promoting its CW rotation. Aspartate binding to Tar inhibits CheA-to-CheY phosphotransfer, lowering the concentration of CheY-P. This promotes CCW rotation and hence smooth swimming.

The chemotactic excitation is transient. Simultaneous initiation of other processes leads to adaptation back to the prestimulus state. Glutamic acid residues in the Tar cytoplasmic domain are continually methylated and demethylated by the transferase CheR and the esterase CheB respectively. CheB has a regulatory domain, homologous to CheY, which, when phosphorylated by CheA, inhibits its catalytic domain. The resulting net increase in methylation leads to adaptation. CheY-P dephosphorylation is accelerated by CheZ protein. Modulation of CheZ's aggregation state may play a role in adaptation (Blat and Eisenbach, 1994; Eisenbach, 1996) and/or signal amplification (Wang and Matsumura, 1996).

Received for publication 12 August 1998 and in final form 18 November 1998.

Address reprint requests to Dr. Shahid Khan, Department of Physiology and Biophysics, Albert Einstein College of Medicine, Bronx, NY 10461. Tel.: 718-430-4046; Fax: 718-430-8819; E-mail: skhan@aecom.yu.edu.

0006-3495/99/03/1706/14 $2.00

Chemotactic excitation and subsequent adaptation may be separated in time by monitoring responses to rapid changes in chemoeffector concentration. This has been accomplished for free-swimming bacteria by mixing (Macnab and Koshland, 1972) and flash photolysis of photosensitive "caged" chemoeffectors (Khan et al., 1993). Concentration changes effected by flow-cell exchange (Berg and Tedesco, 1975) and iontophoresis (Segall et al., 1982) were used to study responses of bacteria tethered by a single flagellum to glass coverslips. Adaptation times of responses to the large step stimuli studied by such methods ranged from tens of seconds to minutes and were proportional to fractional changes in receptor occupancy (Spudich and Koshland, 1975). When chemoeffector concentrations were changed enzymatically (Brown and Berg, 1974) or ramped (Block et al., 1983), such that both excitation and adaptation contributed to the response, the response amplitude was proportional to the rate of change of receptor occupancy.

Only flash photorelease and iontophoresis were sufficiently rapid for direct measurement of the subsecond signal processing or excitation times. Excitation kinetics measured by flash photorelease and iontophoresis were similar for responses that saturated (i.e., produced completely smooth-swimming populations). However, there were discrepancies in response sensitivity, as assessed from the amplitudes of subsaturation responses. A response latency, evident in the iontophoretic measurements, was not observed upon flash photorelease of serine or protons (Khan et al., 1993, 1995). The present study was undertaken to provide a more detailed description of chemotactic response kinetics and resolve these discrepancies.

MATERIALS AND METHODS

Caged compounds

New caged compounds, caged HPTS, the *O*-1-(2-nitrophenyl)ethyl ether of 8-hydroxypyrene-1,3,6-tris-sulfonic acid, caged L-aspartate (Scheme 1), and the P^3-2,6-dinitrobenzyl ester of ATP (2,6-dinitrobenzyl-caged ATP) were synthesized for these studies. Caged HPTS is a nonfluorescent compound that on photolysis releases fluorescent HPTS. This fluorescence was used to measure the extent of caged HPTS photolysis and thus to calibrate the photolysis apparatus. The intermediate leading to HPTS at a rate with constant k_{HPTS} is an *aci*-nitro compound (Barth et al., 1997, and references therein). Caged L-aspartate also photolyzes via an *aci*-nitro intermediate that has a broad absorption band. Its exponential decay with rate constant k_{asp} probably determines the rate of L-aspartate formation (Corrie and Trentham, 1993). The nitrosoketone by-products react with thiols and were rendered biologically inert by including dithiothreitol (DTT) in the solution, as done previously for other caged chemoeffectors (Khan et al., 1993).

Synthesis and properties of caged HPTS

The approach used to synthesize caged HPTS has been described by Walker et al. (1989). The hydrazone of 2-nitroacetophenone (311 mg (1.76 mmol)) was quantitatively oxidized to 1-(2-nitrophenyl)diazoethane. Ddiazoethane (1.45 mmol) in 7.3 ml $CHCl_3$ was added to 1 mmol of the trisodium salt of HPTS (pyranine; Lancaster Synthesis, Morecombe, England) dissolved in 5 ml H_2O at pH 4.86. The mixture was shaken vigorously in a stoppered flask for 4 h at 21°C. At this time, absorption spectra indicated that 22% of the HPTS remained, and the pH had risen to 5.2. The pH was adjusted to 4.4 with aqueous HCl, and a further 0.3 mmol diazoethane was added in 1.5 ml $CHCl_3$. The shaking was continued for a further 5 h, at the end of which 8% of the HPTS remained. The reaction mixture was then partitioned between $CHCl_3$ and water at pH 7.8. The aqueous phase was loaded onto a DEAE cellulose column (2.5 cm diameter × 50 cm) and eluted with a 4-liter gradient of 0.01–1.01 M TEAB (triethylammonium bicarbonate) at pH 7.4 and 5°C.

After some minor impurities, HPTS eluted as a broad peak (centered at 0.68 M TEAB) fairly well resolved from caged HPTS (centered at 0.8 M TEAB) and an unknown contaminant at >0.9 M TEAB. HPTS was distinguished from caged HPTS because only the former absorbs at 454 nm (ϵ 2.01×10^4 M^{-1} s^{-1} at pH > 8). This absorbance was used to identify and discard aliquots of caged HPTS containing HPTS. The unknown contaminant had an absorption band at 373 nm. It was identified as present in the eluate when the ratio of absorption at 403 nm to that at 373 nm was less than 1.23. For caged HPTS this ratio was 1.28. Tubes containing pure caged HPTS were pooled and evaporated to dryness in vacuo several times after addition of methanol to the dried material to remove TEAB. The tris-triethylammonium salt of caged HPTS was obtained in 70% overall yield from HPTS and stored in the dark at −20°C in aqueous solution. Quantification was based on ϵ 1.85×10^4 M^{-1} s^{-1} at λ_{max} 403 nm in aqueous solution near neutrality (pH 6–8).

Q_p, the product quantum yield of caged HPTS on photolysis was measured by comparison with that of the P^3-1-(2-nitrophenyl)ethyl ester of ATP (caged ATP), using the approach described by Walker et al. (1989). In a typical experiment a cuvette containing 0.10 mM caged HPTS, 0.10 mM caged ATP, 2 mM dithiothreitol, and 50 mM ammonium phosphate buffer at pH 7.0 and 22°C was illuminated with a xenon arc lamp for various times through a UG11 320 (± 40)-nm bandpass filter. Samples of the solution were analyzed by fluorescence and/or absorption spectroscopy at pH 10 to detect formation of HPTS (ϵ 2.01×10^4 M^{-1} s^{-1} at 454 nm, a wavelength at which caged HPTS does not absorb) and by high-performance liquid chromatography (HPLC) (Whatman Partisil SAX) to measure formation of ATP and decay of caged HPTS and caged ATP (HPTS was retained on the column), using aqueous 0.54 M $(NH_4)H_2PO_4/(NH_4)_2HPO_4$ at pH 5.5 and acetonitrile (10% by volume) as the eluting solvent.

The rate of photolysis of caged HPTS was measured by recording the absorption or fluorescence changes associated with the formation of HPTS after flash photolysis (20-μs pulse of a Candela dye laser at 320 nm) (Walker et al., 1988).

Synthesis and properties of caged aspartate (β-2,6-dinitrobenzyl ester of L-aspartic acid)

N-*t*-BOC-α-*t*-butyl L-aspartate (Sigma Chemical Co., St. Louis, MO) (0.5 mmol) was treated with 1 mmol KF and 0.5 mmol 2,6-dinitrobenzyl bromide under reflux in dry acetone for 4 days. The reaction was followed by thin-layer chromatography on K6F plates, monitoring the appearance of a UV-absorbing spot. The *t*-BOC ester was purified by flash chromatography. After removal of solvent the product was treated with 5 ml trifluoroacetic acid for 1 h at 22°C and rotary evaporated to dryness, followed by 4 evaporations with methanol. Caged aspartate was obtained in 68% yield, stored in the dark at −20°C in methanol, and assayed from ϵ 12,000 M^{-1} cm^{-1} at λ_{max} 230 nm. Amino acid analysis of material, redissolved in water at pH 3 after evaporation of methanol, contained 1.4% aspartic acid.

2,6-Dinitrobenzyl esters are prone to spontaneous hydrolysis in aqueous solution at a rate proportional to hydroxide ion concentration. The rate of caged aspartate hydrolysis was 1.1×10^{-4} min^{-1} at 22°C and pH 7.0. During an experiment it was kept in solution on ice wrapped in foil until required, so as to minimize hydrolysis.

Q_p of caged aspartate was also measured by comparison with caged ATP. First the 2,6-dinitrobenzyl chromophore was compared with that of the 1-(2-nitrophenyl)ethyl group, the photolabile moiety of caged ATP and caged HPTS, in the wavelength range transparent to the UG11 bandpass filter. The spectra are almost identical from 335 nm to 360 nm, but from 300 nm to 335 nm the 2,6-nitrobenzyl group only absorbs ~75% as effectively on average. This difference was ignored because the illumina-

Scheme 1.

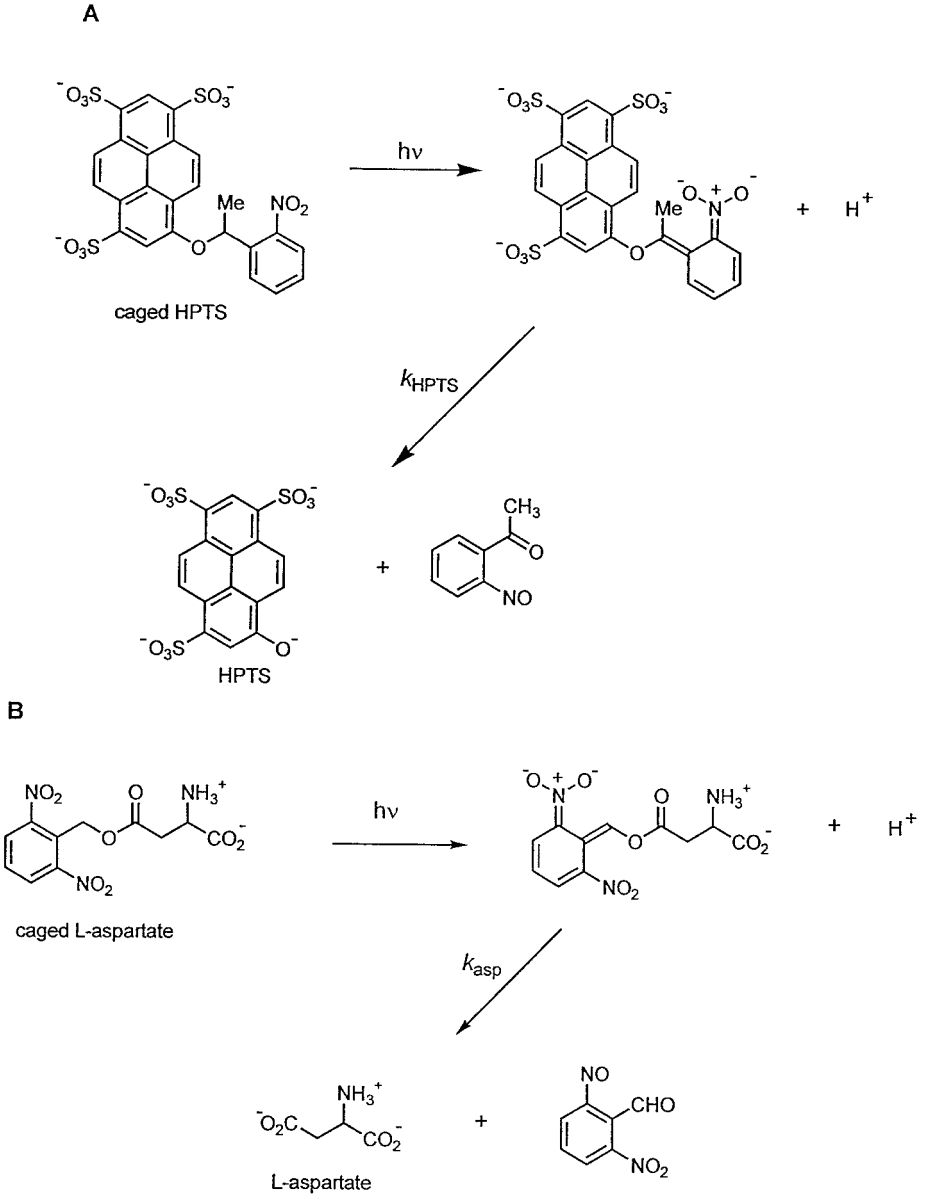

tion for photolysis used in the microscope assays was similar to that used for spectroscopic measurements. The photolysis protocol was as used above for caged HPTS, except that analysis was by HPLC, using a Merck RP8 reverse-phase column with aqueous 5 mM $KH2PO_4/K_2HPO_4$ at pH 5.6 and methanol (10% by volume) as the eluting solvent. Caged ATP, caged aspartate, ATP, and the byproduct of caged aspartate photolysis were monitored at 254 nm to follow the photolysis. The photolysis of caged HPTS and caged aspartate was also compared directly because the aspartate photoreleased in the biological assays was measured from the fluorescence of HPTS generated by caged HPTS photolysis. Similar spectroscopic and HPLC analytical methods (RP8 reverse phase column) were used as when comparing caged HPTS and caged aspartate with caged ATP.

The rate of photolysis of caged L-aspartate was inferred from the rate of decay of the *aci*-nitro intermediate formed after flash photolysis (Walker et al., 1988), using the same apparatus as for caged HPTS.

Synthesis and properties of the P^3-2,6-dinitrobenzyl ester of ATP (2,6-dinitrobenzyl-caged ATP)

2,6-Dinitrophenyldiazomethane was prepared from the parent aldehyde according to the methods of Walker et al. (1989). 2,6-Dinitrobenzyl-caged ATP was synthesized from ATP and the diazomethane in a mixed $CHCl_3$/water solvent at pH 4 and then isolated in 15% overall yield, using DEAE anion exchange chromatography and preparative reverse-phase HPLC. 2,6-Dinitrobenzyl-caged ATP had $Q_p = 0.6$ when measured against caged ATP as standard (see comment above on Q_p measurement of 2,6-dinitrobenzyl compounds). On flash photolysis ATP formed at 10 s^{-1} at 22°C, 0.2 M ionic strength, and pH 7, as measured by the rate of decay of the *aci*-nitro intermediate.

Growth and preparation of bacteria

E. coli strains RP437 (wild type for motility and chemotaxis) and RP2361 (Tar deletion mutant) were obtained from Dr. J. S. Parkinson. Overnight cultures were prepared from bacteria that were motility selected on tryptone soft agar (0.35% agar). Inocula (1/100) of the overnight cultures were grown at 35°C in tryptone broth (plus 20 μg/ml streptomycin). The bacteria were harvested in late exponential phase ($OD_{600\ nm} \approx 0.5\ cm^{-1}$). They were washed three times with buffer A (20 mM Na_2HPO_4/KH_2PO_4, pH 7.0 $\pm$ 0.2, 10 mM potassium chloride, 0.1 mM EDTA, 5 mM lithium

lactate, 125 μM methionine). For caged aspartate experiments, buffer A contained, in addition, 5 mM DTT.

For tethered-cell experiments, the bacteria were sheared (27-gauge needles) after the first wash, then washed two more times. The washed bacteria were incubated with flagellar antibody-coated circular (22 mm) coverslips for ~30 min. The coverslips were mounted on a laminar flow cell (Berg and Block, 1984). Untethered bacteria were subsequently washed out by buffer A.

Mixing experiments

A custom-made mixing apparatus was utilized. This consisted of two reservoirs, one filled with buffer A containing aspartate and the other with buffer A containing bacteria, which fed into a 10-μl mixing chamber. The mixed solution was pulled via valve (PS3; Pharmacia Biotech, Uppsala, Sweden) through the laminar flow cell observation chamber with a peristaltic pump (Gilson minipuls II) at a rate of 0.03 ml/s. The mixing ratio and wash-in/wash-out times of the mixed suspensions were determined by mixing HPTS solutions of known concentration with buffer A. Mixing was accomplished within 0.1 s. The transit time between mixing and exchange into the chamber was 7 $\pm$ 1 s at the flow rate used. Higher (more than fivefold) flow rates impaired the motility of the bacteria, probably because of breakage of flagella. Flow was stopped for motility measurements by simultaneously turning off the pump and closing the valve controlling entry to the flow cell.

Photorelease assays

Photolysis of caged HPTS was used to measure the energy of the photolyzing flash and, thus, estimate the amounts of caged chemoeffectors, here aspartate, photolyzed in behavioral assays. The fluorescence of known concentrations of HPTS (Molecular Probes, Eugene, OR) in aqueous 0.1 M phosphate buffer at pH 7.0 was used to construct a calibration curve for determination of amounts of caged HPTS photolyzed in the microscope. A 450 $\pm$ 15-nm exciter/510-nm dichroic/>520-nm barrier filter cassette was used for excitation and visualization of HPTS fluorescence. The intensity was recorded using a photodiode (Thorlabs model 201/579-7227) connected to a current-to-voltage amplifier (Oriel 70710), digital readout (Oriel 70701), and a chart recorder (Pharmacia REC101). Alternatively, video records were made and fluorescence intensities obtained upon digitization (Khan et al., 1993). From the fluorescence released on photolysis of caged HPTS, the amount of aspartate released was calculated.

Two modes with different geometries were used to effect photolysis of caged chemoeffectors in microscope behavioral assays (Khan et al., 1993). In one mode, light from a Gert-Rapp flash lamp was transmitted through a UG11 filter with infrared reflective coating and directed onto the sample at an angle of 40 $\pm$ 2° via a liquid light guide that terminated in a plano-convex lens. The collimated beam from the lens illuminated all or most of the sample. In the other mode, shuttered episcopic Kohler illumination from a continuous mercury arc lamp (Nikon), also directed through the UG11 filter, effected photolysis over a local area comparable to the microscopic field of view as seen through the eyepieces. Distinction between diffusion out of the video field of view and photobleaching of released HPTS was achieved by varying the viscosity of the solution with glycerol. Viscosity of HPTS/glycerol buffers was measured using a Cannon-Ubbelohde (size 100) viscometer. The bacteria were imaged using a long working distance objective (32× magnification, 0.5 numerical aperture) when photorelease was effected by direct side illumination from a flash lamp and by a fluorite phase-contrast objective (40× magnification, 0.85 numerical aperture) when epiillumination effected photorelease. The transmissivity of the fluorite objective (~65% at 360 nm) decreased at lower wavelengths.

For swimming-cell assays, samples of ~5 μl volume were observed in a bridged coverslip chamber through a quartz coverslip positioned on two glass (0.17 mm) coverslips. The quartz coverslips were cleaned in fuming nitric acid before use. This treatment reduced the number of bacteria stuck to the coverslip surface. For tethered-cell assays, the flow cell was used. After bacteria were introduced, buffer with caged aspartate was introduced and 10 min was allowed for equilibration before flash photorelease.

The free aspartate contamination in the caged aspartate was also determined using a bioassay based on CheB mutants. CheB mutants have abnormally long adaptive recovery times (Clarke and Koshland, 1979). Recovery times of *Salmonella typhimurium* SL4041 CheB mutant strain upon mixing with known aspartate concentrations were measured. A calibration curve constructed from these measurements was used to read off the aspartate concentration from the responses observed when the mutant bacteria were mixed with samples of caged aspartate. The contamination level was 1.5%, in correspondence with values determined after synthesis, implying that degradation during subsequent handling was negligible.

Addition of D-aspartate, a nonmetabolizable analog, was used to increase prestimulus receptor occupancy, which was always nonzero because of L-aspartate contamination of the caged sample. The gain (g) provided a measure of response strength. This, as defined previously (Khan et al., 1993), was Δ(motor bias)/ΔR_{occ}; where Δ(motor bias), the change in {CCW/(CW + CCW)}rotation bias, was estimated from the change in the rate of change of direction (Δrcd), given Δ(motor bias) = $-(0.0012)\Delta rcd$ (figure 2 of Khan et al., 1993).

Motion analysis

Video records were digitized off-line (VP320 digitizer, ExpertVision version 1.4 software; Motion Analysis, Santa Rosa, CA) and analyzed as previously described (Khan et al., 1993, 1995). A zoom lens coupled to the video camera was used to adjust the final magnification such that one pixel in the digitized image spanned 0.5 μm. For each concentration change, the aggregate response of >1000 bacteria was measured: a single flash sequence typically captured responses of 50–100 bacteria. Swimming cell records were batch-processed at 30 and 15 frames/s for measurement of excitation response ($t_{1/2}$) and adaptation recovery (t_r) times, respectively. These were the times required for a half-maximum response and recovery back to prestimulus behavior, respectively (Khan et al., 1995). Excitation response data were expressed as the response rate, k_{ex}, where $k_{ex} = \ln 2/t_{1/2}$. Because at 15 frames/s, linear speed (*spd* operator) as well as the frame-to-frame angular speed (*rcd* operator) is sensitive to changes in swim-tumble behavior (Sager et al., 1988; Khan et al., 1993), the *rcd/spd* ratio, as well as the *rcd* alone, was used to measure recovery times. Under our experimental conditions, unstimulated wild-type bacteria typically had a population *rcd* between 750 and 850°/s. This corresponded to a {CCW/(CW + CCW)} motor rotation bias of 0.7 and 0.6, respectively. Excitation responses were fitted by single exponentials, using nonlinear least-squares curve-fitting routines available in SIGMAPLOT (Jandel Scientific) software. Nonlinear least-squares procedures were also used to infer K_D's by fitting models to the recovery time data obtained in mixing experiments. For estimation of peak response amplitudes and recovery times, successive 10-frame (i.e., 0.33 s) windows were averaged. The number of windows used for determination of peak response amplitude depended on the duration of the postexcitatory period before initiation of adaptive recovery.

For tethered-cell experiments, the unavoidable presence of stuck cells precluded batch processing of the video data. Single tethered bacteria were boxed out and digitized individually at 60 frames/s. One pixel spanned 0.3 μm in the digitized images. Analysis was limited to bacteria with rotation rates under 20 Hz. *Avel* and *ngdr* operators were used to compute the angular velocity and monitor regularity of rotation. The *avel* is the first derivative of the direction of travel with respect to time. The *ngdr* is the ratio of the distance from the first point in the path to the given point over the actual path distance from the first point to the given point. The rotation sense, given by the sign of the *avel*, was subsequently extracted. Individual cell path files were then merged to yield the time dependence of the population change in motor rotation bias.

RESULTS

Spectroscopy and photochemistry of caged compounds

The extent of caged aspartate photolysis relative to that of caged HPTS when the compounds were exposed to near-UV light in a cuvette was used to estimate the aspartate concentration jumps delivered in microscope photorelease assays. Caged HPTS has a pH-independent absorption spectrum over the 4–10 pH range and is not fluorescent (Fig. 1). The excitation spectra of HPTS overlap with its absorption spectra in the 350–500-nm range. The invariance of the emission spectra in the 4–10 pH range is due to the fact that the pK_a of the excited state is ~1 (Parker, 1968).

The extents of caged aspartate and caged HPTS photolysis relative to that of caged ATP were 33% and 20%, respectively. In separate experiments, direct comparison of caged aspartate and caged HPTS photolysis confirmed the expected ratio of 1.6 (33%/20%) within a ±20% error range. Q_p, the number of product molecules divided by the number of photons absorbed at a particular wavelength or, as here, wavelength range was 0.63 for caged ATP (Walker et al., 1988, 1989). Thus the Q_p's for caged aspartate and caged HPTS are 0.21 and 0.13, respectively. The estimated Q_p for caged HPTS does not take into account absorption of near-UV photons by the pyrene ring system as well as by the 1-(2-nitrophenyl)ethyl chromophore. However, this does not affect the calibration of the extent of caged aspartate photolysis using caged HPTS. Proton release studies on photolysis of 2,6-dinitrobenzyl acetate (Nerbonne, 1986) suggested O_p values for 2,6-dinotrobenzyl carboxylate esters are significantly greater than those of 1-(2-nitrophenyl) ethyl esters. By contrast, O_p valves for 2,6-dinitrobenzyl and 1-(2-nitrophenyl) ethyl caged ATPs were within 10% of one another.

The rates of photolysis of caged HPTS and caged aspartate were measured from the appearance of the absorption or fluorescence of HPTS and from the decay of the *aci*-nitro intermediate, respectively (Fig. 2). The rates of formation of HPTS and aspartate were 550 s^{-1} and 630 s^{-1}, respectively, at pH 7.0, 0.1 M ionic strength, and 22°C. They were approximately proportional to proton concentration over the 5–9 pH range.

Stimulus characteristics

The two microscopy set-ups for photolysis of caged aspartate had distinct characteristics and uses. Fifteen percent of caged HPTS was photolyzed, using shuttered episcopic illumination, from a 30-ms exposure of the continuous mercury arc lamp. The fluorescence of the photoreleased HPTS decayed after a lag phase of ~5 s (Fig. 3 *A*). The decay was due to diffusion of HPTS out of the field of view, as it was suppressed by making the solution more viscous (15 cp), a condition that decreased diffusion by over an order of magnitude. The lag was due to the fact that the diameter of the video field of view was one-third that of the area over which the sample was photolyzed, so that initial diffusion did not affect the observed fluorescence. In this mode, photobleaching of HPTS was significant (>10% s^{-1}), as evaluated using HPTS/glycerol buffers. This has been corrected for in Fig. 3 *A*. Thus episcopic-illumination-based photolysis generated concentration jumps that decayed after a few seconds. Therefore, it was used for measurement of excitation responses, but not for analysis of subsequent adaptation.

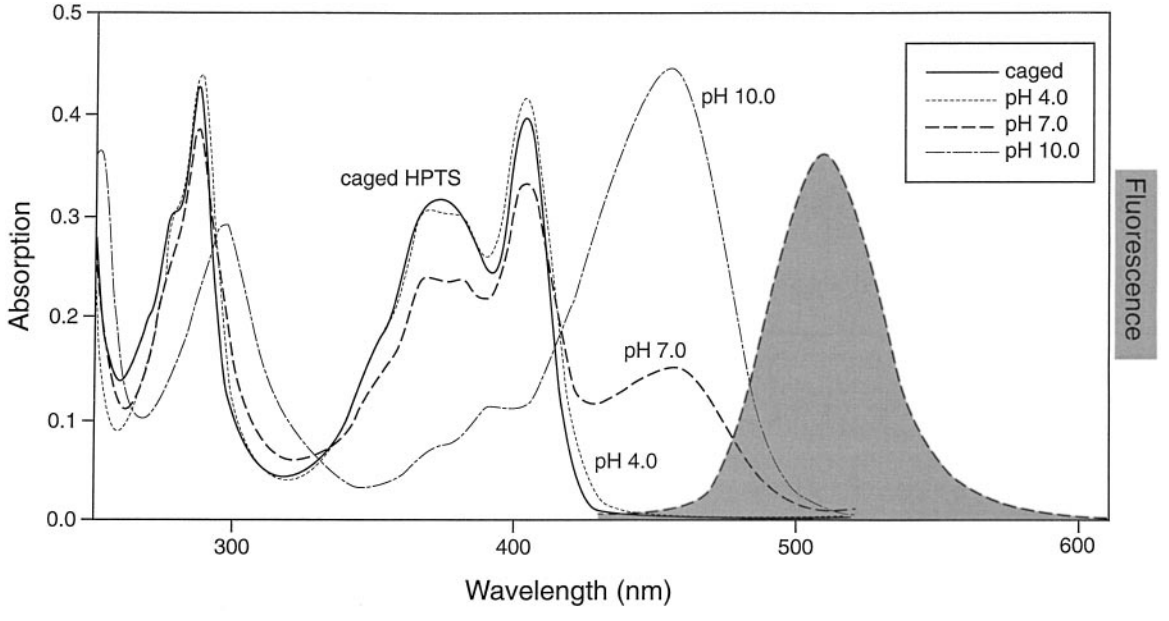

FIGURE 1 Spectra of HPTS and caged HPTS. Absorption spectra of 21.2 μM caged HPTS at pH 7.0 and 22.5 μM HPTS at pH values as indicated, measured in a 1-cm-path cell. The fluorescence spectrum is that of HPTS (λ_{ex} 403 nm) at pH 7.0. Caged HPTS is not fluorescent under these conditions.

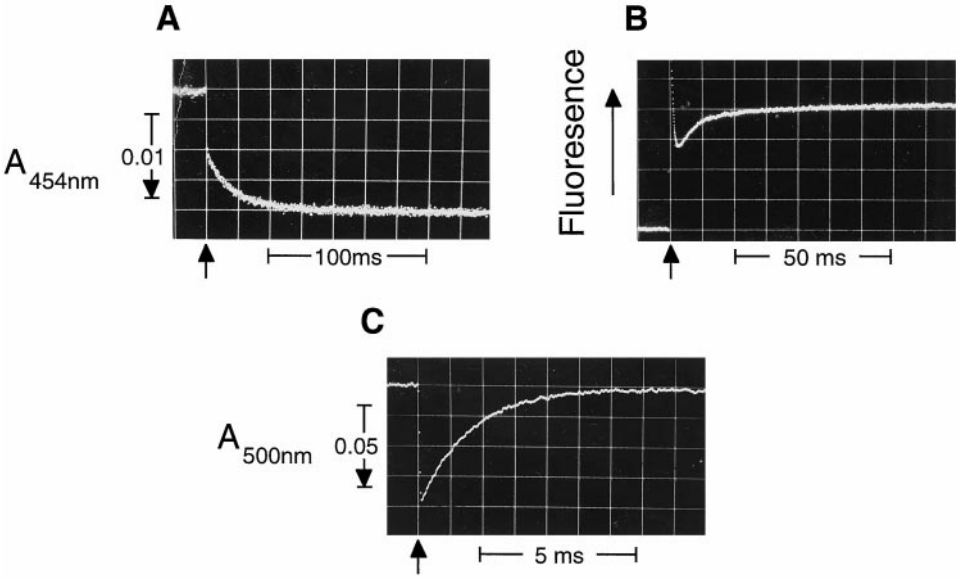

FIGURE 2 Absorption and fluorescent transients on photolysis of caged compounds. (*A*) Absorbance change at 454 nm on photolysis of caged HPTS at pH 7.9. The aqueous solution contained 0.53 mM caged HPTS, 0.10 M KCl, 2 mM dithiothreitol, and 10 mM 1,3-bis(tris(hydroxymethyl)-methylamino)propane adjusted to pH 7.9 with aqueous HCl. (*B*) Fluorescence change upon photolysis of caged HPTS at pH 7.5. The aqueous solution contained 0.1 mM caged HPTS. KCl (0.1 M), 2-mercaptoethanol (2 mM), and HEPES (20 mM) were adjusted to pH 7.5 with aqueous KOH. The fluorescence was excited through a 406 (± 30)-nm bandpass filter and detected with a Kodak 15 (510-nm cutoff) filter. (*C*) Absorption change at 500 nm on photolysis of caged aspartate. The aqueous solution contained 0.1 mM caged aspartate, 2 mM dithiothreitol, and 50 mM potassium phosphate at pH 7.0. All experiments were performed at 22°C in a 4-mm square cuvette. Fluorescence was excited through the cuvette base. Arrows mark the time of the 20-μs laser pulse.

On the other hand, when the light from the xenon flash illuminated most of the sample via a light guide, the concentration of photoreleased HPTS over the video field of view remained constant for ~1 min. This is illustrated by the 30-s record shown (Fig. 3 *B*); the slight decrease in fluorescence is due to photobleaching (~1% s^{-1}) and not to diffusion of HPTS out of the video field of view, because alteration of the viscosity of the solution was without effect. A portion (2.4 ± 0.4%) of a 50–500 μM caged HPTS sample was typically photolyzed per flash at standard operating voltage (200 V). This set-up could therefore be used to measure adaptation as well as excitation responses, but was not as suitable as episcopic illumination for producing aspartate jumps giving a large ΔR_{occ}.

Aspartate concentration dependence of chemotactic recovery times

The fractional change in aspartate (Tar) receptor occupancy (ΔR_{occ}) provided a measure of stimulus strength. ΔR_{occ}'s were taken to be proportional to adaptive recovery times (t_r's), which were measured directly in mixing experiments. $\Delta R_{occ} = (t_r/t_{rmax})$, where t_{rmax} was the maximum recovery time obtained at saturating aspartate concentrations. Equations of the form $\Delta R_{occ} = (1/x) \cdot \Sigma_{x=1-n}([Asp]/([Asp] + K_D^x)$, where x is the number of distinct affinities, were used to infer K_D's. The dependence of t_r on aspartate concentration was biphasic (Fig. 4). Recovery times depended steeply on aspartate concentration over the 0.5–5 μM range. They continued to increase, albeit less steeply, over the 10–100 μM range. The initial steep concentration dependence, but not the latter increase, was consistent with the 1.2 μM K_D for aspartate binding to Tar measured in isolated membrane preparations (Biemann and Koshland, 1994). Best fits (coefficient of determination, $r^2 = 0.69$) to the data using a 1.2 μM single site predicted a t_{rmax} value only two-thirds of that observed and attained 90% of this value at 12 μM aspartate, also contrary to observation. The K_D for the best fit to an arbitrary single-site model was 10.5 ± 1.5 μM ($r^2 = 0.74$). Assumption of a low-affinity binding site in addition and equimolar to the 1.2 μM high-affinity site determined from the biochemical data significantly improved the fit. The K_D for the low-affinity site determined from the best fit ($r^2 = 0.9$) to the two-site model was 74 ± 8 μM. Operationally, therefore, two binding sites with K_D's of 1.2 and 70 μM were used to compute receptor occupancies for subsequent experiments.

Measurement of swimming cell responses

Smooth-swimming responses of wild-type (RP437) bacteria have been identified at the level of individual cells on photorelease of a chemoattractant (Khan et al., 1992). Population responses, as measured by the *rcd*, have been related to change in motor rotation bias through analysis of smooth-swimming and tumbly mutant populations (Khan et al., 1993). Here we place limits on the measurement precision

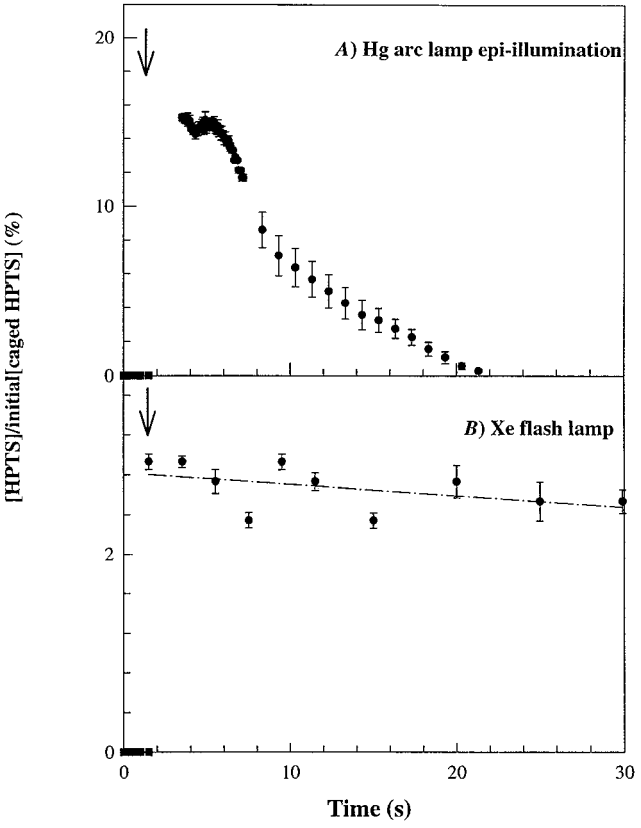

FIGURE 3 Calibration of photoreleased stimuli. Shown are averaged ($n = 3$) fluorescence versus time plots for fields of view where HPTS was photoreleased by exposing the following: (*A*) An area comparable to the field of view with 30-ms shuttered epiillumination from a mercury arc lamp focused through a fluorite 40× objective. A second or so was required to change filter cassettes to monitor HPTS fluorescence after the near-UV epiillumination flash (hence the gap in the record). (*B*) The sample was exposed to ~1 ms-side illumination from a xenon flash lamp through a light guide. Photobleaching depended upon the objective used; was proportional to transmissivity, power, and numerical aperture; and is corrected for in *A* but not *B* (see text). Arrows denote times of flash.

of responses of a single, few, or many bacteria to attractant photorelease.

Just as on serine photorelease (Khan et al., 1992), strong smooth-swim responses of single wild-type bacteria to aspartate photorelease were identified. Path trajectories became smoother, reflecting a drop in *rcd*, and the average distance between centroids lengthened per unit time, reflecting the increase in *spd*. However, it was not possible to reliably detect responses at the level of individual cell paths, when the population response was far from saturation.

Next, small populations were analyzed. Examples of saturating and subsaturating responses of eight bacteria populations are shown (Fig. 5 *A*). Even for saturating responses, temporal resolution was lowered by the smoothing of data necessary to define initiation of the response. The problem was worse for subsaturating responses.

In contrast, when population size was large ($n > 2000$), measurement of subsaturation, as well as saturation responses, was achieved without loss of temporal resolution and with high sensitivity (Δ *rcd* = 50 corresponding to Δ(motor bias) of 0.05). Subsaturation as well as saturation excitation responses followed exponential decay kinetics, indicating the absence of a response latency (Fig. 5 *A*, *iii* and *iv*). In addition, the excitation and early adaptive recovery phase for subsaturation responses could be fitted by a sum of two exponentials, one negative and the other positive.

The increased precision reflects the effect of population size on the frame-to-frame standard deviation, σ_T, of the population *rcd*. Provided individual cell paths have similar σ (variance σ^2), σ_T is expected to be $\sigma/n^{1/2}$, where n is the number of paths. Fig. 5 *B* shows this to be so. σ_T was independent of x, the number of frames averaged, where one frame takes 33 ms, provided that xn corresponded to an interval greater than 2.7 s. n ranged from 1000 to 2000 paths in all subsequent data records shown, unless otherwise stated. As a result, time-resolved and reproducible measurement of subsaturation responses was achieved.

Criteria for distinguishing a subsaturating from a saturating response were established. A sample was determined to exhibit a subsaturation response if the population *rcd* at peak response, rcd_{peak} ($\pm$ standard error of the peak, σ_p) was greater than rcd_{sat} by $(\sigma_p^2/x_p + \sigma_s^2)^{1/2}$, where x_p is the number of frames averaged to determine the peak response. σ_s is the standard error of the mean saturation response. rcd_{sat} and σ_s were determined by recording responses of the experimental cultures obtained upon mixing with serine (1 mM). Upon mixing, the population *rcd* decreased to an rcd_{sat} ($\pm$ standard error, σ_s) of 360 $\pm$ 63°/s (three experiments), a value similar to that measured for smooth-swimming mutant strains lacking chemotaxis protein components (figure 5 of Khan et al., 1995). There was a second semiquantitative determinant of subsaturation. For responses that were just detectible, the dwell time at the peak response before adaptive recovery was <1 s but increased progressively with increasing response strength. For responses that just saturated, several seconds elapsed before initiation of adaptive recovery.

The responses observed were triggered specifically by Tar-aspartate binding. Mutants deleted for Tar, the aspartate receptor, did not respond to aspartate jumps producing up to $0.4\Delta R_{occ}$ change. Wild-type bacteria did not respond to photolysis of 1 mM 2,6-dinitrobenzyl-caged ATP, showing that the photolysis byproducts did not act on Tar.

Comparison of threshold swimming- and tethered-cell responses

Excitation responses of *E. coli* to L-aspartate have been measured previously using iontophoretic delivery to cells tethered to glass by a single flagellum (Segall et al., 1982). Therefore, responses of swimming and tethered cells to photorelease of L-aspartate were compared. Single cultures were split in half. One half was used for measurement of swimming-cell responses; the other half was sheared for measurement of tethered-cell responses. The response

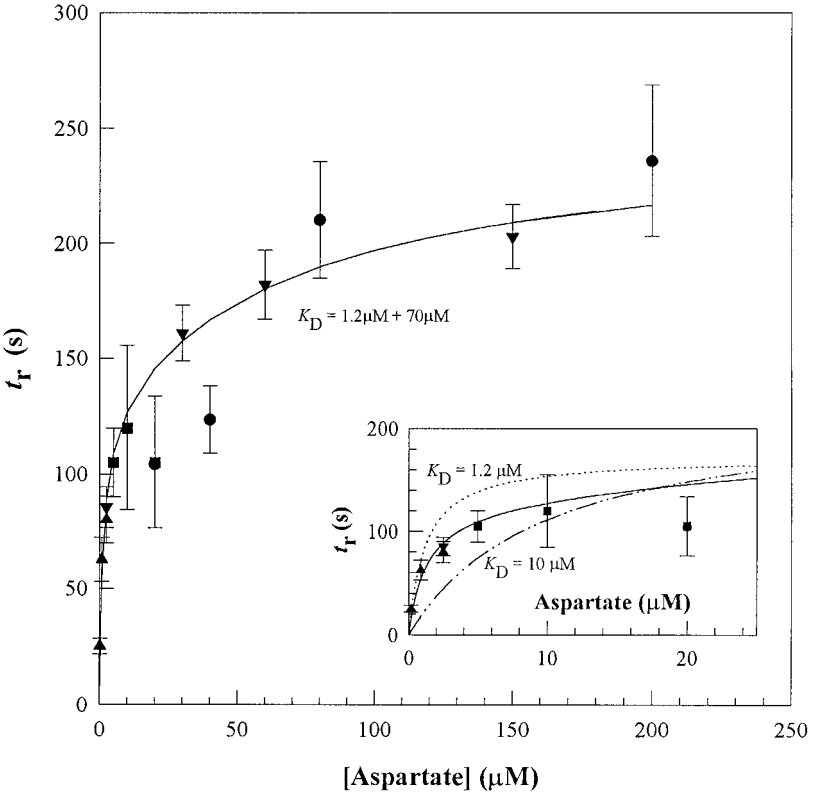

FIGURE 4 Dependence of adaptation times on aspartate concentration. Different symbols denote different cultures. Recovery times at different concentrations were normalized to times obtained upon jumps of 20 μM aspartate. Recovery times to jumps of 1 and 10 mM aspartate were 280 ($\pm$ 24) and 302 ($\pm$ 16) s, respectively, indicating saturation in this concentration regime. The solid line represents a high (1.2 μM) and low (70 μM) affinity fit to the data. (*Inset*) Goodness of fit of the two-site model (*solid line*) compared to 1.2 μM (*dotted line*) and best-fit (10 μM) (*dashed-dotted line*) single-site models. Fits were made to all of the data but are shown for the 0–20 μM aspartate concentration range, where differences were most evident. Values predicted for the 1.2 μM and 10 μM single-site models were systematically higher and lower, respectively, than the observed data. In addition, whereas the 10 μM single-site model fitted the data beyond 20 μM adequately, the 1.2 μM model failed to account for the continuing increase in t_r beyond 20 μM.

threshold for swimming and tethered cells was the same. Responses were measurable down to a 0.004 change in ΔR_{occ}. This corresponded to an 11 nM aspartate concentration jump from a prestimulus background concentration of 60 nM. Responses over a fourfold ΔR_{occ} change above this threshold had comparable sensitivity and kinetics. Pooled data from two such experiments are shown (Fig. 6).

Responses of tethered cells to large step attractant stimuli producing solely CCW rotation for many tens of seconds have been observed to exhibit an "overshoot" period of enhanced CW rotation before achieving poststimulus steady state (Berg and Tedesco, 1975). This seems to have been a peculiarity specific to the large stimulus response regime, because it was not observed in the present experiments; the motile behavior of both swimming and tethered cell populations decayed monotonically back to the steady state. As documented in the literature (Spudich and Koshland, 1976), there was a large variation in both unstimulated rotation bias as well as adaptive recovery times of tethered bacteria. This and the small sample size contributed to greater uncertainty regarding the completeness and duration of adaptive recovery (t_r) for the tethered bacteria. The swimming cell record, however, showed that adaptation was complete (Fig. 6).

Tethered-cell responses to photoreleased aspartate also did not show a response latency. Therefore, the 0.23–0.9-s latencies observed upon iontophoretic stimulation (table 1 in Segall et al., 1982; figure 2 in Segall et al., 1986) do not appear to be due to increased mechanical load or differences in chemoeffector/receptor species. For $\Delta R_{occ} = 0.01$, tethered as well as swimming cell responses were almost twofold more rapid than the most rapid responses recorded for iontophoretically delivered step stimuli (Segall et al., 1982).

Stimulus strength dependence of adaptation recovery times

Recovery times remained proportional to stimulus strength (ΔR_{occ}) over the measurable range. The observed dependence was comparable to that determined for known aspartate concentrations in mixing experiments (Fig. 7). This comparison provided an independent measure of amounts of aspartate liberated in photorelease assays. The congruence showed that estimates derived from photolysis of caged HPTS were accurate within 20% experimental error.

One concern was that recovery back to prestimulus behavior may result not only from chemotactic adaptation, but also from depletion of photoreleased aspartate from the medium due to uptake by the bacteria. In the latter case, the rate of depletion of aspartate from the medium would depend upon the density of bacteria in the experimental sample. However, recovery times were insensitive to more than fivefold variation in bacterial cell density. Similarly, the density of the bacteria was at least an order of magnitude less in tethered versus swimming cell experiments; yet recovery times were similar. Thus recovery times were governed exclusively by chemotactic adaptation. Estimation of the extent of uptake from the binding and rate data available for *E. coli* aspartate transport (Kay, 1971; Schellenberg and Furlong, 1977) indicated a negligible reduction in the medium aspartate

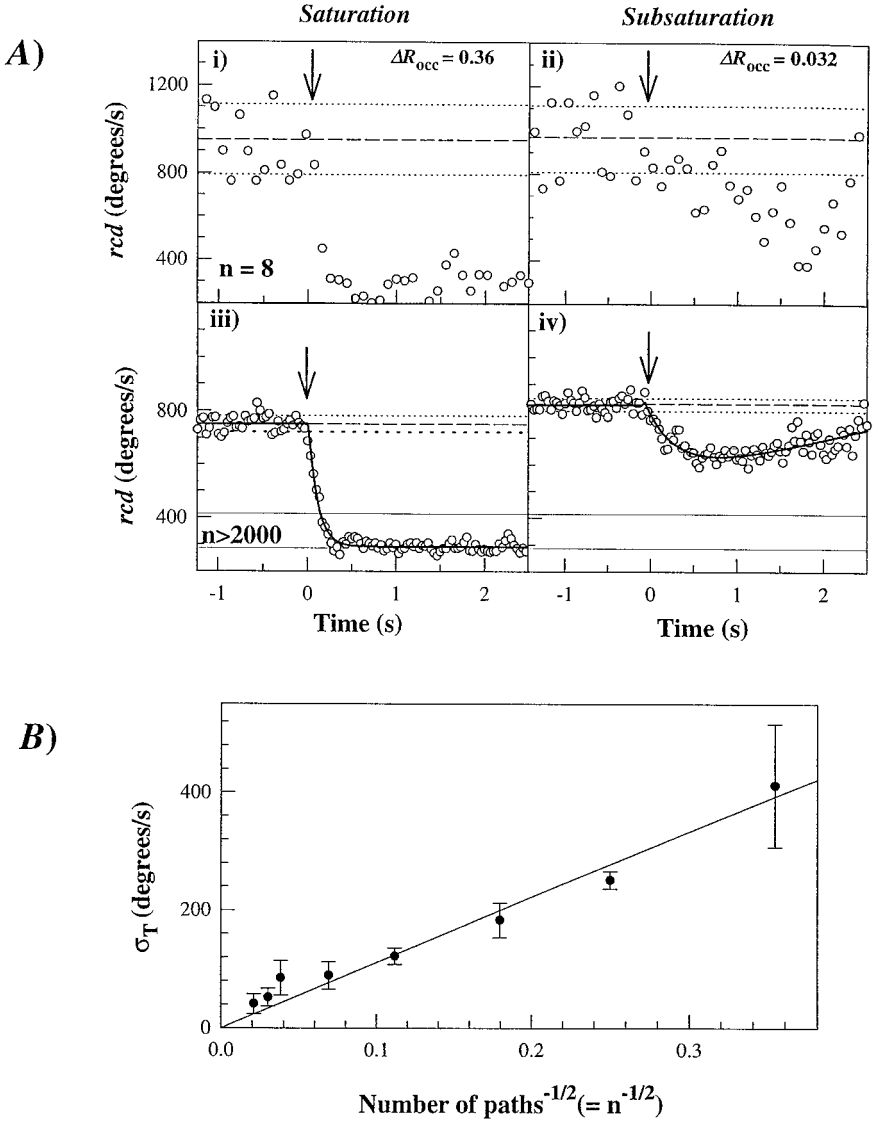

FIGURE 5 Swimming-cell responses to jumps of photoreleased aspartate. (*A*) Saturation (*i* and *iii*) and subsaturation (*ii* and *iv*) responses of populations of 8 (*i* and *ii*) and >2000 bacteria (*iii* and *iv*). The temporal resolution of the 8-path files is one-third that of the >2000 path files. The data in *iii* and *iv* were fitted by single and double exponentials, respectively. For *iii*, excitation response rate, k_{ex} = 9.5 (± 0.9) s^{-1}. For *iv*, k_{ex} = 2.8 (± 0.6) s^{-1}; gain, g = 7.7 (± 1.2). Arrows denote photolyzing flashes. The prestimulus *rcd* mean and the mean (± frame-to-frame SD) are denoted by dashed and dotted lines, respectively. Solid lines denote rcd_{sat} (± error). (*B*) Standard deviation, σ_T (± error), of the path population *rcd* as a function of population size, *n*. Thirty frames/s digitization rate.

concentration (<1%/min) over the time scale of the experiments, consistent with these observations.

All experimental samples contained a prestimulus background of L-aspartate, present as a contaminant in the caged sample. The prestimulus background, and hence receptor occupancy, R_{occ}, was increased by the addition of D-aspartate, a nonmetabolizable analog. Recovery times obtained upon mixing the bacteria with L- and D-aspartate to final concentrations of 10 μM and 375 μM, respectively, were similar. Thus prestimulus R_{occ} for 375 μM D-aspartate was ~0.5. The ratio of the D- and L-aspartate concentrations was similar to the biochemically determined ratio of the K_D's of these ligands for Tar (D/L = 40 μM/1.2 μM = 33; Dunten and Koshland, 1991). The second-site D-aspartate K_D was presumably large (70 × 40/1.2) and inconsequential for the R_{occ} obtained at 375 μM. Cultures with the higher prestimulus R_{occ} adapted more rapidly than cultures with lower receptor occupancy. This trend is consistent with the occupancy-dependent increase in kinetics of receptor methylation, the process underlying chemotactic adaptation (Springer et al., 1979; Shapiro and Koshland, 1994). Population recovery times, however, varied significantly from culture to culture. Therefore, further work will be required to assess the significance of the observed difference.

Stimulus strength dependence of excitation response times

Response times ($t_{1/2}$) were estimated directly by taking the mean of the data points clustered, within one standard error, around the *rcd* value corresponding to the half-maximum response. They were also obtained as the reciprocal of the rate, $k_{ex} = (\ln 2)/t_{1/2}$, obtained from single exponential fits to the data. Although there was agreement between values obtained from the two procedures, the latter provided a more accurate measure as well as an estimate of the error. The ability to obtain well-determined excitation responses from single cultures enabled examination of the culture-to-

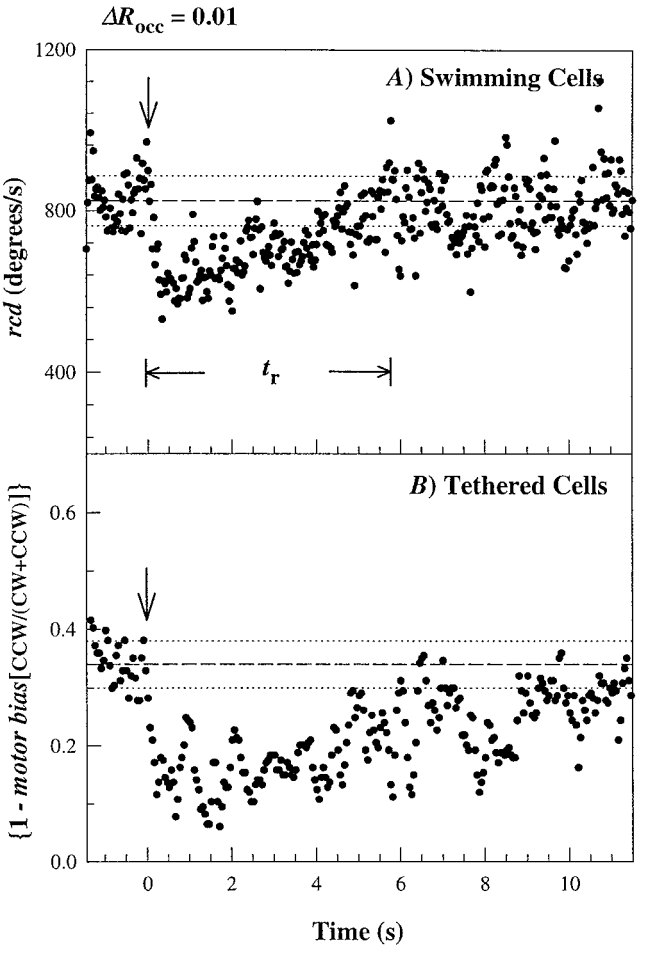

FIGURE 6 Comparison of swimming- and tethered-cell responses. Stimulus strength, ΔR_{occ} = 0.01. Arrows indicate photolyzing flashes. (*A*) Swimming cells (500–1000 cell paths). k_{ex} = 6.9 (±1.2) s^{-1}, g = 19.7 (±7.7). t_r is ~6 s. The prestimulus *rcd* mean and the mean (± frame-to-frame SD) are denoted by dashed and dotted lines, respectively. (*B*) Tethered cells (n = 8 cells, 5 flashes/cell). k_{ex} = 7.4 (± 3.5) s^{-1}, g = 22.5. t_r is between 7 and 12 s. The prestimulus mean and the mean (± frame-to-frame SD) of the motor rotation bias are denoted by dashed and dotted lines, respectively.

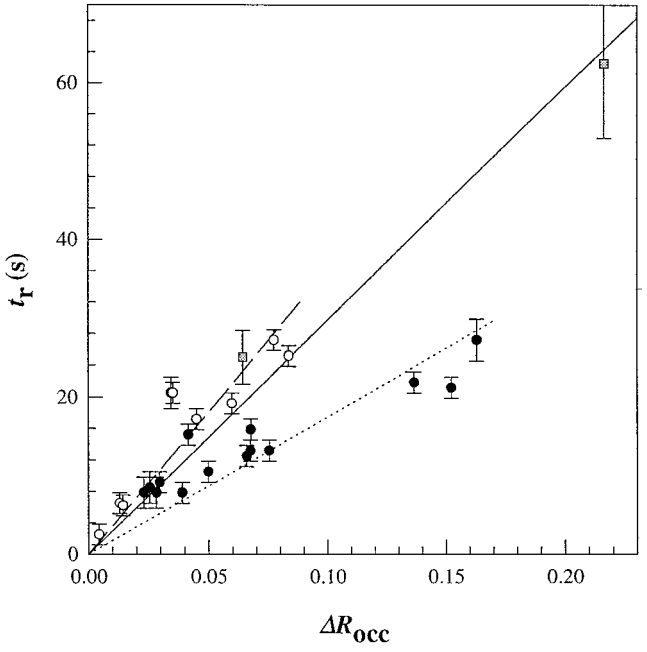

FIGURE 7 Adaptation recovery times (t_r's) to small step stimuli. Stimulus strength (ΔR_{occ}) dependence at low (○, – – –) and high (●, ·····) prior receptor occupancy. This was increased by the addition of D-aspartate (375 μM). Data from the mixing experiments (▨, ——) are superimposed. See Fig. 4 for complete data from the mixing experiments.

culture variability. This variability was significant. For similar ΔR_{occ}'s, rates obtained from different cultures differed by as much as a factor of 2.

A plot of excitation response rate, k_{ex}, versus stimulus strength, ΔR_{occ} (Fig. 8), showed, importantly, that responses near threshold had kinetics comparable to that of saturation responses. The rate increased slightly with increasing stimulus strength. The mean value over 0.01–0.2ΔR_{occ} range was 4.66 ± 0.87 s^{-1}; over the 0.25–0.4ΔR_{occ} range, it was 9.35 ± 1.71 s^{-1}. Higher prior receptor occupancy resulted in more rapid chemotactic excitation responses. It was estimated, using available biochemical data (Dunten and Koshland, 1991), that half of the receptor sites were occupied upon addition of 375 μM D-aspartate. With added D-aspartate the mean k_{ex} value was 8.01 ± 0.08 s^{-1} over the 0.01–0.2ΔR_{occ} range (Fig. 8).

DISCUSSION

The flash photorelease assay has been developed in a number of ways. In earlier work, amounts photoreleased were estimated by following pH changes due to photorelease of protons with fluorescent pH indicator dyes (Khan et al., 1993). For such estimates, use of weakly buffered solutions, whose buffering capacity had to be measured separately, was necessary. Here, a caged fluorophore (see Corrie and Trentham, 1995, for a brief review of caged fluorophores), which had the advantage that it was nonfluorescent before photolysis, was used. Caution must be exercised when caged HPTS is used because HPTS will photobleach under intense irradiation (Kolyar et al., 1996). Besides estimation of the extent of caged aspartate photolysis, caged HPTS was also valuable in that upon photolysis its fluorescent photoproduct HPTS could be used to estimate the diffusion-induced efflux of molecules of comparable size out of the video field of view (Fig. 3). The 2,6-dinitrobenzyl caged group for amino acids has a significant advantage for kinetic studies over the carbamoyl group used previously (Khan et al., 1993), because of the rapidity of photolysis as inferred from the *aci*-nitro decay rate. However 2,6-dinitrobenzyl esters are susceptible to slow hydrolysis at neutral pH.

The measurement precision of swimming cell responses was evaluated. Comparison of swimming and tethered cell responses showed that chemotactic responses did not depend on differences inherent in the two assays, namely mechanical load and flagellar bundle hydrodynamics. Response recovery, as well as excitation, was measured. Li-

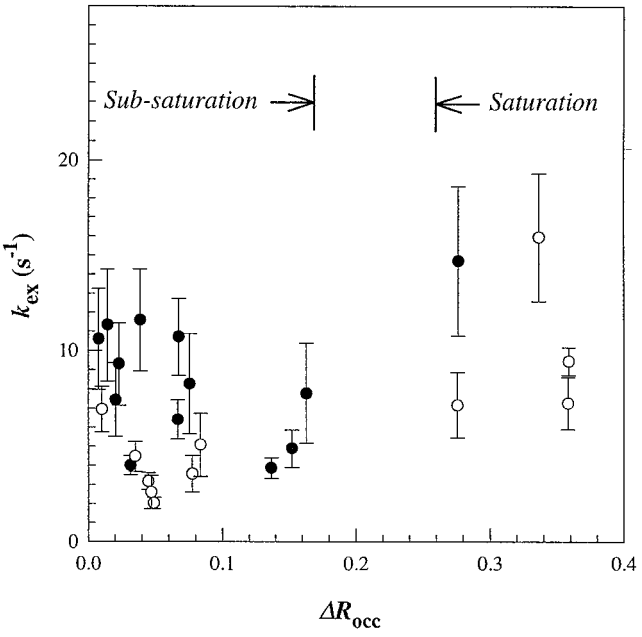

FIGURE 8 Excitation response rate, k_{ex}, versus stimulus strength, ΔR_{occ}. Data with high (●, +375 μM D-aspartate) and low (○) prior receptor occupancy. Rate constants and their standard errors were estimated by least-squares single-exponential fits to the data. ΔR_{occ} values for which responses with subsaturation amplitudes (see text) were obtained are indicated.

gand-receptor binding affinities were operationally defined by measurement of adaptive recovery times to step stimuli applied by mixing known aspartate concentrations with the bacteria. Recovery times to jumps generated by photorelease measured chemotactic adaptation, as they matched recovery to similar size step stimuli obtained by mixing and, furthermore, did not depend on bacterial cell concentration. These experiments establish the photorelease assay as a quantitative, sensitive assay for time-resolved analysis of bacterial chemotactic responses.

New information has been obtained from the analysis regarding both adaptation and excitation kinetics as discussed below.

Adaptation kinetics

The dependence of recovery times on aspartate concentration seen in the mixing experiments (Fig. 4) was not compatible with biochemical studies showing a single site K_D of 1.2 μM. It was best fit by two binding affinities. Most simply, this suggests that a second aspartate binding site in *E. coli* Tar may be occupied, but with much weakened affinity, because of the negative cooperativity, as in *Salmonella typhimurium* Tar (Biemann and Koshland, 1994) or *E. coli* Tsr (Lin et al., 1994). A 70 μM K_D is sufficiently weak to have escaped detection in the biochemical binding studies. Second-site binding was also not evident in ^{19}F-NMR studies of the isolated ligand-binding domain (Danielson et al., 1994). However, changes at the second site induced upon binding of aspartate to the first site may be more severe in the isolated domain.

The correspondence of chemotactic recovery times with biochemically determined sugar-periplasmic protein binding isotherms first established the paradigm that recovery times were proportional to fractional change in receptor occupancy (Spudich and Koshland, 1975). Later, recovery times (Clarke and Koshland, 1979) or the analogous transition times (Berg and Tedesco, 1975) could be similarly fitted by using binding affinities to the MCPs estimated from membrane vesicle preparations or inferred from other behavioral assays (Mesibov et al., 1973), respectively. The swimming cell studies required use of tumbly *che* mutants and of large stimuli ($t_r > 25$ s) for ease of quantification, whereas tethered cell transition times measured only incomplete adaptation. Use of computer-assisted motion analysis obviates the need for mutants, and the increased precision and temporal resolution enables accurate quantification of short recovery times. In photorelease experiments, recovery times to small ($< 0.1\Delta R_{occ}$) stimuli remained proportional to stimulus size, even though the proportionality constant varied somewhat, depending upon prior receptor occupancy. Neither tethered or swimming cell responses showed "overshoot" (Berg and Tedesco, 1975). The proportionality between recovery times and stimulus size has been thought to be a consequence of the global control of CheB methylesterase activity (Kehry et al., 1985), ensuring that the number of receptor complexes that serve as substrates for CheR remain invariant with stimulus size, so that CheR continues to operate at the maximum rate. It is not known whether together, or in addition to, receptor methylation, some other process such as CheZ oligomerization (Eisenbach, 1996) controls adaptation in the small stimulus regime examined here. In any case, inference of a second weak affinity binding site follows from the mixing data, given acceptance of the paradigm. Strong negative cooperativity in ligand/transducer binding is one strategy for extending the chemotactic response range. The present study provides behavioral evidence to indicate that bacteria may implement this strategy generally for MCP-based signaling.

Other explanations are possible for our behavioral data. Two or more distinct aspartate affinities could be due to different populations of receptors generated as a result of heterogeneous clustering and/or methylation. The possibility that there is just a single aspartate affinity, but one that is shifted to a higher value than 1.2 μM, perhaps due to CheA-CheW-MCP associations, seems less likely based on fits to the mixing data (Fig. 4), but cannot currently be ruled out. Discrimination among these possibilities will require study of an MCP-based signaling system, where affinities of both ligand-binding sites in the MCP dimer have been biochemically determined. Thus ΔR_{occ}'s obtained based on the (t_r/t_{rmax}) ratio cannot be given a simple physical interpretation but provide, because of this, a model-independent measure of stimulus strength.

Excitation kinetics

The excitation amplitude responses of tethered and swimming cells to flash photorelease of aspartate were similar. Responses were detectable at ΔR_{occ}'s as low as 0.004. If a response threshold exists, it is below the detection capability ($\Delta rcd \sim 50$) of the assay. Response amplitudes close to the detection limit were independent of whether aspartate jumps were delivered by iontophoresis (Segall et al. 1986) or by flash photorelease, providing similar estimates of the gain. However, the change in *rcd*, and hence in motor rotation bias, for responses elicited by aspartate jumps producing ΔR_{occ}'s of 0.01 (Fig. 6) and 0.032 (Fig. 5) were similar. In other words, the gain for the latter stimulus was lower ($\sim$7.3). One possibility is that this reflects culture-to-culture variability. Alternatively, or in addition to culture-to-culture variability, the stimulus-response relation may be nonlinear. The lower sensitivity reported for serine was also computed for responses to intermediate stimulus strengths (Khan et al., 1993). It was significant that saturation responses (i.e., 0.4Δ(motor bias)) were not observed below ΔR_{occ} values of 0.15 (Fig. 8). If gain were constant, given that $\Delta R_{occ} = 0.01$ elicits a half-maximum (i.e., 0.2) change in Δ(motor bias) (Fig. 6), $\Delta R_{occ} > 0.02$ should elicit saturation motor responses, contrary to observation. This stimulus-response relation will be analyzed in detail elsewhere.

Excitation response kinetics were comparable to those measured previously for serine. No latency was evident, even for responses close to threshold. It is possible that the latency observed in iontophoretic studies of tethered bacteria reflects a permeation barrier for iontophoresed ligands through the outer membrane porins. It was argued, reasonably enough, that the insensitivity of the observed latent period to concentration, over most of the range examined, ruled out ligand binding as rate limiting (Segall et al., 1982). However, this result would also be obtained if transport across the outer membrane were limited by the number of open porin pores (Delcour, 1997). At very low concentrations, the flux per pore would fall below its saturating value and the "latency" would increase, which is what was observed (Segall et al., 1982). Alternatively, nonresponsive motors might constitute a greater fraction of the sample for close-to-threshold responses, thereby artifactually increasing the mean "latency." The effect of nonresponsive motors would, in contrast, be damped out in a response of a swimming bacterium, which contains contributions from all motors driving propulsion of the flagellar bundle ($\sim$6/bundle). Solely CCW (hence nonresponsive) motors, which constitute a significant fraction of a wild-type sample in tethered cell assays, were not analyzed. However, normally responsive motors that drove bacteria that rotated too rapidly ($>$20 Hz) or bumped into neighboring objects were also excluded from analysis. Poorly responsive and solely CCW-rotating flagella would, in contrast, all contribute to swimming cell responses, which therefore provide a more unbiased measure of the population response.

The absence of a latency indicates that excitation times are limited by decay of intracellular CheY-P pools and CheY-motor associations, with upstream signal-generating receptor reactions being fast. This result is consistent with the known biochemistry. Aspartate-Tar associations-dissociations and coupled conformational changes in the isolated ligand-binding domain occur on a millisecond time scale, as monitored by ^{19}F-NMR (Danielson et al., 1994). The aspartate first-site K_D's of the isolated domain and intact receptors are the same. Thus the simplest possibility is that the conformational transitions in receptor complexes that couple ligand binding to inhibition of CheA activity are also rapid on the excitation time scale.

The decay of intracellular CheY-P pools would be determined by the sum of the phosphorylation (k_1) and dephosphorylation (k_2) rate constants (Fig. 9 *A*). CheY-P constitutes $<$20% of the total CheY in wild-type bacteria, estimated based upon analysis of mutant phenotypes and in vitro phosphotransfer rates (Bray and Bourret, 1995). Therefore, decay of CheY-P pools would be dominated by k_2, as $k_1 < 0.2k_2$ and can only decrease further upon stimulation with chemoattractant. An apparent dephosphorylation rate, k_2, of 10 s^{-1}, estimated from knowledge of intracellular CheZ concentration and measured in vitro rates of CheY auto- and CheZ-accelerated dephosphorylation (Fig. 9 *A*), is compatible with the observed excitation response rates (Fig. 8).

In the simplest models, ligand binding acts solely to shut off CheA kinase activity (Hess et al., 1988), affecting only the phosphorylation rate, k_1. Therefore, such models predict that excitation response kinetics should decrease, albeit little, with stimulus strength. However, instead of a slight decrease, a slight increase with stimulus strength is observed (Fig. 8). This increase may reflect cooperativity in CheY-motor reactions. Such cooperativity will enable a small drop in [CheY-P] to produce a large change in motor bias. The peak change in [CheY-P] levels would be greater at higher stimulus strengths, and accordingly the drop in [CheY-P] required to attain half-maximum changes in motor bias will be achieved more rapidly. Alternatively, or in addition, mechanisms may exist to simultaneously activate CheY-P dephosphorylation, as well as inhibit CheY phosphorylation. A modest activation, consistent with reported values, can account for our data (Fig. 9 *B*). The substantial variability in CheZ-catalyzed CheY-P dephosphorylation rates reported in the literature (5×10^5 M^{-1} s^{-1} (Wang and Matsumura, 1996) to 10^8 M^{-1} s^{-1} (Huang and Stewart, 1993)) may reflect heterogeneity in CheZ activity due to oligomerization (Eisenbach, 1996) or interaction with receptor signaling complexes (Wang and Matsumura, 1996). This heterogeneity may also underlie the observed culture-to-culture variability observed for excitation response rates. Finally, it cannot currently be determined whether changes in CheY-motor occupancy track the decrease in [CheY-P] levels or partially limit response times. The latter, if true, could also explain the observed stimulus strength dependence of excitation response kinetics.

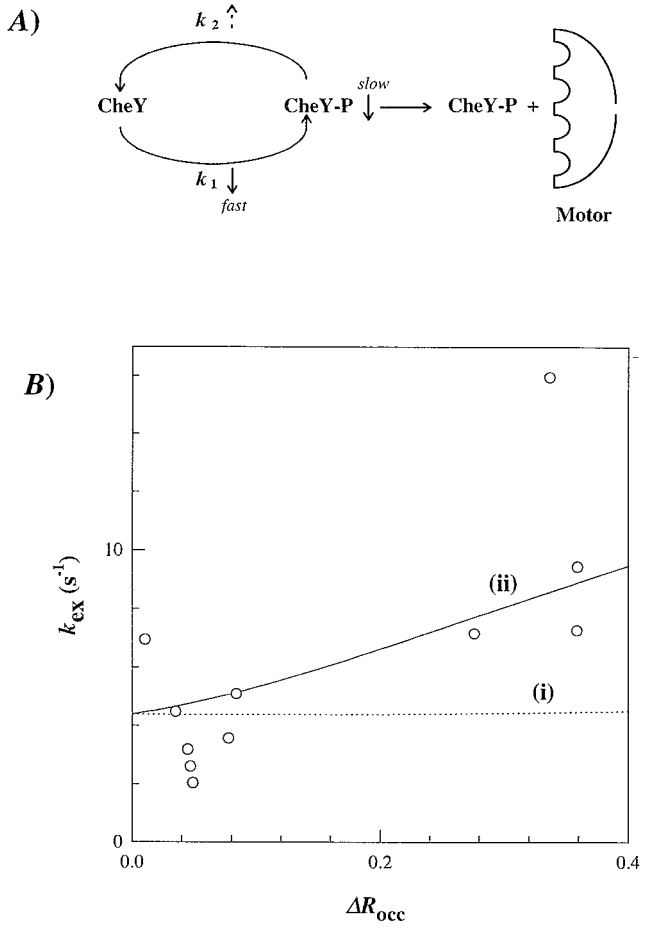

FIGURE 9 (*A*) Smooth-swim signal processing. Absence of a response latency implies that signal generation by receptor complexes is fast relative to downstream events, namely, decay of intracellular CheY-P pools and CheY-P-motor complexes. Decay rate, $d[\text{CheY-P}]/dt = k_1[\text{CheY}] - k_2[\text{CheY-P}]$, where t is time, k_1 and k_2 are post-stimulus phosphorylation and dephosphorylation rate constants respectively. Integration yields $[\text{CheY-P}] = C\{1 - \exp(-(k_1 + k_2)t)\} + [\text{CheY-P}]_{t=0}\exp(-(k_1 + k_2)t)$, where $C = k_1[\text{CheY}_T]/(k_1 + k_2)$, $[\text{CheY-P}]_{t=0}$ = prestimulus [CheY-P], $[\text{CheY}]_T$ = total intracellular [CheY]. Thus, [CheY-P] decay depends on the sum of k_1 and k_2. $k_2 = k_0 + k_3$ [CheZ], where the CheY-P autophosphatase rate, $k_0 = 0.05\ s^{-1}$ (Lukat et al., 1991). The CheZ accelerated CheY-P phosphatase rate, $k_3[\text{CheZ}] = 10\ s^{-1}$, given $k_3 = 5 \times 10^5\ M^{-1}\ s^{-1}$ (Lukat et al., 1991) and [CheZ] = 20 μM (Matsumura et al., 1990). Hence $k_2 = 10.05\ s^{-1}$. Che Y-P = 1.6 μM when CheY_T = 10 μM (Bray and Bourret, 1995). Therefore, $k_1 = k_2[\text{CheY-P}]/[\text{CheY}] = (10.05\text{x}1.6)/8.4 = 2.0\ s^{-1}$. (*B*) Predicted fits of excitation response kinetics versus stimulus strength (ΔR_{occ}). Under our experimental conditions, the motor bias $B = \{\text{CCW}/(\text{CW} + \text{CCW})\}$ varied between 0.6 and 0.8. The value of 0.6 was taken as the limiting value. Computed changes in [CheY-P] were converted to changes in motor bias using the equation $B = 1.5[\text{CheY-P}]_{t=0}/(1.5[\text{CheY-P}]^H_{t=0} + [\text{CheY-P}]^H)$ (Bray and Bourret, 1995), where H = the Hill coefficent for CheY-motor interaction. Time-dependent changes in CheY-P at various ΔR_{occ}'s were simulated using parameters listed above. $k_{t=0}$'s are prestimulus rate constants. (*i*) Dotted line: Ligand binding only affects k_1. Poststimulus rate, $k_1 = k_{1(t=0)}(1 - \Delta R_{occ})$, given complete abolition of CheA activity upon ligand binding. (*ii*) Continuous line: Ligand binding activates k_2 in addition to abolishing CheA activity ($k_1' = k_{1(t=0)}(1 - \Delta R_{occ})$). $k_2 = k_{0(t=0)} + k_3(A) + k_{3(t=0)}(1 - A) + (k_3 - k_{3(t=0)})(\alpha\beta\Delta R_{occ})$; where $k_3' = 10k_{3(t=0)}$; [receptor]/[CheZ], α = 0.1; CheZ copies bound per receptor, β = 6 (Wang and Matsumura, 1996); prestimulus inactivated CheZ fraction, A = 0.95; H = 5.5 (Kuo and Koshland, 1989).

In conclusion, the form, magnitude, and stimulus strength dependence of the measured excitation response kinetics all indicate that smooth-swim signal processing is controlled by decay of intracellular CheY-P pools. To discriminate between possible models of smooth-swim signal generation, it will be important to quantitate excitation responses to stimuli greater than those employed in the present study. High-speed video digitization techniques are currently under development for a such purpose.

We thank Fred Castellano for expert technical assistance in the early phases of this project and Robert Macnab for advice on construction and operation of the mixing apparatus.

Supported by grants from the National Institutes of Health (GM43919 to SK) and the North Atlantic Treaty Organization (CRG940021 to SK/DRT).

REFERENCES

Appleby, J. L., J. S. Parkinson, and R. B. Bourret. 1996. Signal transduction via the multi-step phosphorelay: not necessarily a road less traveled. *Cell.* 86:845–848.

Barth, A., J. E. T. Corrie, M. J. Gradwell, Y. Maeda, W. Mantele, T. Meier, and D. R. Trentham. 1997. Time-resolved infrared spectroscopy of intermediates and products from photolysis of 1-(2-nitrophenyl)ethyl phosphates: reaction of the 2-nitrosoacetophenone byproduct with thiols. *J. Am. Chem. Soc.* 119:4149–4159.

Berg, H. C. 1983. Movement of self-propelled objects. *In* Random Walks in Biology. Princeton University Press, Princeton, NJ. 59–73.

Berg, H. C., and S. M. Block. 1984. A miniature flow cell designed for rapid exchange of media under high-power microscope objectives. *J. Gen. Microbiol.* 130:2915–2920.

Berg, H. C., and D. A. Brown. 1972. Chemotaxis in *Escherichia coli* analyzed by three-dimensional tracking. *Nature.* 239:500–504.

Berg, H. C., and P. M. Tedesco. 1975. Transient response to chemotactic stimuli in *Escherichia coli. Proc. Natl. Acad. Sci. USA.* 72:3235–3239.

Biemann, H-P., and D. E. Koshland, Jr. 1994. Aspartate receptors of *Escherichia coli* and *Salmonella typhimurium* bind ligand with negative and half-of-the-sites cooperativity. *Biochemistry.* 33:629–634.

Blair, D. F. 1995. How bacteria sense and swim. *Annu. Rev. Microbiol.* 49:489–522.

Blat, Y., and M. Eisenbach. 1994. Phosphorylation-dependent binding of the chemotaxis signal molecule CheY to its phosphatase, CheZ. *Biochemistry.* 33:902–906.

Block, S. M., J. E. Segall, and H. C. Berg. 1983. Adaptation kinetics in bacterial chemotaxis. *J. Bacteriol.* 154:312–323.

Bray, D. 1998. Signaling complexes: biophysical constraints on intracellular communication. *Annu. Rev. Biochem. Biomol. Struct.* 27:59–75.

Bray, D., and R. B. Bourret. 1995. Computer analysis of the binding reactions leading to a transmembrane receptor-linked multiprotein complex involved in bacterial chemotaxis. *Mol. Biol. Cell.* 6:1367–1380.

Brown, D. A., and H. C. Berg. 1974. Temporal stimulation of chemotaxis in *Escherichia coli. Proc. Natl. Acad. Sci. USA.* 71:1388–1392.

Clarke, S., and D. E. Koshland, Jr. 1979. Membrane receptors for aspartate and serine in bacterial chemotaxis. *J. Biol. Chem.* 254:9695–9702.

Cochran, A. G., and P. S. Kim. 1996. Imitation of *Escherichia coli* aspartate receptor signaling in engineered dimers of the cytoplasmic domain. *Science.* 271:1113–1115.

Corrie, J. E. T., and D. R. Trentham. 1993. Caged nucleotides and neurotransmitters. *In* Bioorganic Photochemistry Series, Vol. 2, Biological Applications of Photochemical Switches. H. Morrison, editor. John Wiley and Sons, New York. 243–305.

Corrie, J. E. T., and D. R. Trentham. 1995. Synthesis of photoactivatable fluorescein derivatives bearing side chains with varying properties. *J. Chem. Soc. Perkin. Trans.* 1993–2000.

Danielson, M. A., H-P. Biemann, D. E. Koshland, Jr., and J. J. Falke. 1994. Attractant and disulfide induced conformational changes in the ligand binding domain of the chemotaxis aspartate receptor: a ^{19}F-NMR study. *Biochemistry.* 33:6100–6109.

Delcour, A. H. 1997. Function and modulation of bacterial porins: insights from electrophysiology. *FEMS Microbiol. Lett* 151:115–123.

Dunten, P., and D. E. Koshland, Jr. 1991. Tuning the responsiveness of a sensory receptor via covalent modification. *J. Biol. Chem.* 266: 1491–1496.

Eisenbach, M. 1996. Control of bacterial chemotaxis. *Mol. Microbiol.* 20:903–910.

Falke, J. J., R. B. Bass, S. L. Butler, S. A. Chervitz, and M. A. Danielson. 1997. The two-component signaling pathway of bacterial chemotaxis: a molecular view of signal transduction by receptors, kinases, and adaptation enzymes. *Annu. Rev. Cell. Dev. Biol.* 13:457–512.

Falke, J. J., and D. E. Koshland, Jr. 1987. Global flexibility in a sensory receptor: a site-directed cross-linking approach. *Science*. 237: 1596–1600.

Gardina, P. J., and M. D. Manson. 1996. Attractant signaling by an aspartate chemoreceptor dimer with a single cytoplasmic domain. *Science.* 274:425–426.

Gegner, J. A., D. R. Graham, A. F. Roth, and F. W. Dahlquist. 1992. Assembly of an MCP receptor, CheW, and kinase CheA complex in the bacterial chemotaxis signal transduction pathway. *Cell.* 70:975–982.

Hess, J. F., K. Oosawa, N. Kaplan, and M. I. Simon. 1988. Phosphorylation of three proteins in the signaling pathway of bacterial chemotaxis. *Cell.* 53:79–87.

Huang, C., and R. C. Stewart. 1993. CheZ mutants with enhanced ability to dephosphorylate CheY, the response regulator in bacterial chemotaxis. *Biochim. Biophys. Acta.* 1202:297–304.

Kay, W. W. 1971. Two aspartate transport systems in *Escherichia coli*. *J. Biol. Chem.* 216:7373–7382.

Kehry, M. R., T. G. Doak, and F. W. Dahlquist. 1985. Sensory adaptation in bacterial chemotaxis: regulation of demethylation. *J. Bacteriol.* 163: 983–990.

Khan, S., K. Amoyaw, J. L. Spudich, G. P. Reid, and D. R. Trentham. 1992. Bacterial chemoreceptor signalling probed by flash photorelease of a caged serine. *Biophys. J.* 62:67–68.

Khan, S., F. Castellano, J. L. Spudich, J. A. McCray, R. S. Goody, G. P. Reid, and D. R. Trentham. 1993. Excitatory signaling in bacteria probed by caged chemoeffectors. *Biophys. J.* 65:2368–2382.

Khan, S., J. L. Spudich, J. A. McCray, and D. R. Trentham. 1995. Chemotactic signal integration in bacteria. *Proc. Natl. Acad. Sci. USA.* 92:9757–9761.

Kolyar, A. B., N. Borovok, S. Raviv, L. Zimany, and M. Gutman. 1996. Fast redox perturbation of aqueous solution by photoexcitation of pyranine. *Photochem. Photobiol.* 63:448–454.

Kuo, S. C., and D. E. Koshland, Jr. 1989. Multiple kinetic states for the flagellar motor switch. *J. Bacteriol.* 171:6279–6287.

Lin, L. N., J. Li, J. F. Brandts, and R. M. Weis. 1994. The serine receptor of bacterial chemotaxis exhibits half-site saturation for serine binding. *Biochemistry.* 33:6567–6570.

Lukat, G. S., B. H. Lee, J. M. Mottonen, A. M. Stock, and J. B. Stock. 1991. *J. Biol. Chem.* 266:8348–8354.

Macnab, R. M., and D. E. Koshland, Jr. 1972. The gradient sensing mechanism in bacterial chemotaxis. *Proc. Natl. Acad. Sci. USA.* 69: 2509–2512.

Matsumura, P., P. S. Roman, K. Volz, and D. McNally. 1990. Signalling complexes in bacterial chemotaxis *In* Biology of the Chemotactic Response. Symposium 46. J. P. Armitage and J. M. Lackie, editors. Cambridge University Press, Cambridge. 135–154.

Mesibov, R., G. W. Ordal, and J. Adler. 1973. The range of attractant concentrations for bacterial chemotaxis and size of response over this range. Weber law and related phenomena. *J. Gen. Physiol.* 62:203–223.

Milburn, M. V., G. G. Prive, D. L. Milligan, W. G. Scott, J. Yeh, J. Jancarik, D. E. Koshland, Jr., and S-H. Kim. 1991. Three-dimensional structures of the ligand-binding domain of the bacterial aspartate receptor with and without a ligand. *Science.* 254:1342–1347.

Nerbonne, J. M. 1986. Design and application of photolabile intracellular probes. *Soc. Gen. Physiol. Ser.* 40:417–445.

Parker, C. A. 1968. *In* Photoluminescence of Solutions. Elsevier, Amsterdam. 328–344.

Sager, B. M., J. J. Sekelsky, P. Matsumura, and J. Adler. 1988. Use of a computer to assay motility in bacteria. *Anal. Biochem.* 173:271–277.

Schellenberg, G. D., and C. E. Furlong. 1977. Resolution of the multiplicity of the glutamate and aspartate transport systems of *Escherichia coli*. *J. Biol. Chem.* 252:9055–9064.

Segall, J. E., S. M. Block, and H. C. Berg. 1986. Temporal comparisons in bacterial chemotaxis. *Proc. Natl. Acad. Sci. USA.* 83:8987–8991.

Segall, J. E., M. D. Manson, and H. C. Berg. 1982. Signal processing times in bacterial chemotaxis. *Nature.* 296:855–857.

Shapiro, M. J., and D. E. Koshland, Jr. 1994. Mutagenic studies of the interaction between the aspartate receptor and methyltransferase from *Escherichia coli*. *J. Biol. Chem.* 269:11054–11059.

Springer, M. S., M. F. Goy, and J. Adler. 1979. Protein methylation in behavioral control mechanisms and in signal transduction. *Nature.* 280: 279–284.

Spudich, J. L., and D. E. Koshland, Jr. 1975. Quantitation of sensory responses in bacterial chemotaxis. *Proc. Natl. Acad. Sci. USA.* 72: 710–713.

Spudich, J. L., and D. E. Koshland, Jr. 1976. Non-genetic individuality: chance in the single cell. *Nature.* 262:467–471.

Stock, J. B., and M. G. Surette. 1996. Chemotaxis. *In* Escherichia coli and Salmonella: Cellular and Molecular Biology. F. C. Neidhardt, editor. American Society for Microbiology, Washington, DC. 1103–1129.

Walker, J. W., G. P. Reid, J. A. McCray, and D. R. Trentham. 1988. Photolabile 1-(2-nitropenyl)ethyl phosphate esters of adenine nucleotide analogues. Synthesis and mechanism of photolysis. *J. Am. Chem. Soc.* 110:7170–7177.

Walker, J. W., G. P. Reid, and D. R. Trentham. 1989. Synthesis and properties of caged nucleotides. *Methods Enzymol.* 172:288–301.

Wang, H., and P. Matsumura. 1996. Characterization of the $CheA_S$/CheZ complex: a specific interaction resulting in enhanced dephosphorylating activity on CheY-phosphate. *Mol. Microbiol.* 19:695–703.